

Modeling Low Frequency Acoustical Propagation in a Shallow-Water Wedge

Piotr Borejko

TU Wien, Institute of Structural Engineering, Karlsplatz 13, 1040 Vienna, Austria

INTRODUCTION

A 3-D benchmark model of the fluid wedge over an elastic bottom is applied to explain low frequency long-range propagation from an acoustic source submerged in shallow water overlaying a sloping elastic-type seabed.

METHODS/DATA

Acoustical propagation inside the wedge is analyzed into a series of the so-called “generalized ray integrals;” each integral representing a waveform traveling along a specific path in the wedge.

START

RESULTS

This approach provides a complete acoustic signal received at a large distance from the source, including all of the waveforms typical for the model.

CONCLUSION

When a source emits acoustic signals of a low frequency content, the Scholte waves become dominant at large distances.

P1.3-267

Please do not use this space, a QR code will be automatically overlaid



INTRODUCTION

OBJECTIVES

METHODS/DATA

RESULTS

CONCLUSION



Please do not use this space, a QR code will be automatically overlaid

P1.3-267

Introduction [1]: In shallow-water environments long-range propagation proceeds by repeated reflections from the surface and the bottom of the channel, as is the case for underwater sound of a wide spectral range, whose very low frequencies may propagate over large distances (several tens of kilometers), without significant losses.

In this paper, a 3-D benchmark model of the fluid wedge over an elastic bottom (Fig. 1) is applied to explain low frequency long-range propagation from an acoustic source submerged in shallow water overlaying a sloping elastic-type seabed, such as a marine sediment possessing enough rigidity (elasticity in shear), allowing hydroacoustic-to-seismic conversion at a water-sediment interface.

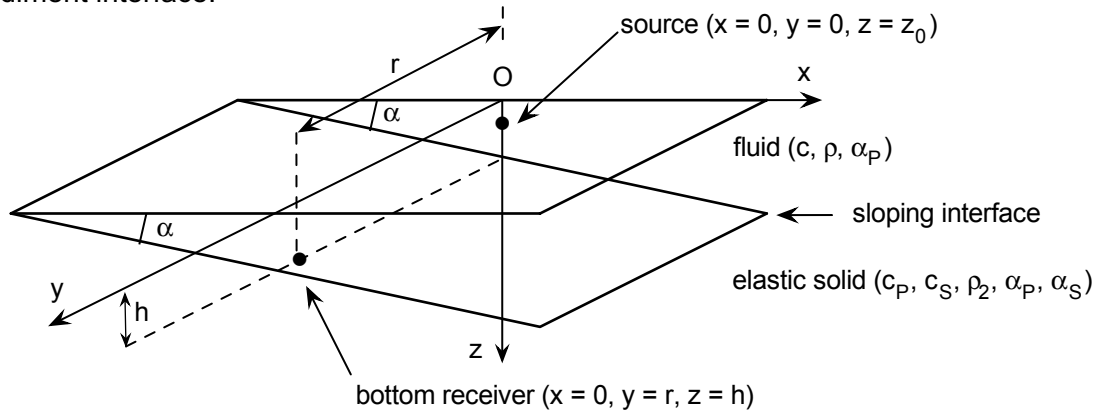


Fig. 1 Fluid wedge over an elastic bottom with a bottom receiver located cross-slope off the source; $\alpha = 3$ deg, $r = 40$ km, $h = 200$ m, $z_0 = 100$ m; fluid (water): $\rho = 1$ g/cm³, $c = 1500$ m/s, $\alpha_p = 0$ dB/ λ , i.e., negligible attenuation of the source signal and the regularly reflected waves; slow-speed elastic bottom (limestone): $\rho_2 = 2.4$ g/cm³, $c_p = 3000$ m/s, $\alpha_p = 0.1$ dB/ λ , i.e., attenuation of the critically refracted wave $\alpha_{\text{Refr}} = \alpha_p$, $c_s = 1460$ m/s, $c_s < c_p$, $\alpha_s = 0.2$ dB/ λ , i.e., attenuation of the Scholte wave $\alpha_{\text{Sch}} = 1.1\alpha_s$.

Generalized-Ray Method [2]: Acoustical propagation inside the wedge, being effected by repeated reflections of the wave emitted from a point source, can be analyzed into a series

$$\bar{\phi} = \bar{\phi}_0 + \sum_{k=1}^N \bar{\phi}_{\pm k}, \quad N = \pi/\alpha, \quad \bar{\phi} = \text{Laplace-transformed velocity potential,}$$

of the so-called “generalized ray integrals”

$$\bar{\phi}_0 = \frac{s\bar{f}(s)}{8\pi^2 c^2} \int_{-\infty}^{+\infty} \int_{-\infty}^{+\infty} S \exp(sg_0) d\xi d\kappa, \quad \bar{\phi}_{\pm k} = \frac{s\bar{f}(s)}{8\pi^2 c^2} \int_{-\infty}^{+\infty} \int_{-\infty}^{+\infty} S \Pi_{\pm k} \exp(sg_{\pm k}) d\xi_{\pm} d\kappa_{\pm l},$$

each integral representing a Laplace-transformed waveform traveling along a specific path in the wedge, the first being the wave from the source directly to the receiver, the second being reflected once, etc.

The inverse Laplace transforms of the ray integrals, found by applying the method of Cagniard,

$$I_0(\tau) = 2\text{Re} \int_0^{q(\tau)} S \frac{dg_0^{-1}}{d\tau} dq, \quad I_{\pm k}(\tau) = 2\text{Re} \int_0^{q(\tau)} S \Pi_{\pm k} \frac{dg_{\pm k}^{-1}}{d\tau} dq.$$

are in the form of single integrals along a complex contour.

Using a standard Gauss-Legendre quadrature

the DGQRUL routine of the IMSL Fortran Numerical Library,

the CPU intensive numerical evaluation of each ray integral can then be accomplished along a new (the analytical equivalent of the original) contour to avoid the branch points of the critically refracted (lateral) waves, the stationary point of the regularly reflected wave, and the pole of the Scholte interface wave. These singular points might cause great difficulty in numerical integration, if performed along the original contour.

The exact solutions for pressure responses (acoustical signals) of the ray integrals are found by applying the convolution theorem. Since the inverse Laplace transforms of the ray integrals are provided at a fixed interval, the convolution integrals are evaluated using Simpson’s rule, and the complete signal recorded by a remote receiver is the sum of the signals corresponding to all ray integrals,

$$p_0(t) = \frac{p_c}{R} \dot{f}(t - r/c) = p_c H(t - t_0) \int_{t_0}^t \ddot{f}(t - \tau) I_0(\tau) d\tau,$$

$$p_c = -\frac{\rho}{4\pi c^2},$$

$$p_{\pm k}(t) = p_c H(t - t_{\pm k}) \int_{t_{\pm k}}^t \ddot{f}(t - \tau) I_{\pm k}(\tau) d\tau,$$

$$p(t) = p_0(t) + \sum_{k=1}^N p_{\pm k}(t), \quad N = \pi/\alpha.$$

The method of generalized ray provides a complete signal recorded by a remote receiver, including all of the three unattenuated waveforms typical for the model: the critically refracted (lateral) waves, the source signal and the regularly reflected waves, and the Scholte interface waves, received in order of their arrivals at a large distance from the source. Note that, for the two in this paper considered Gaussian-weighted source signals, the received levels (RLs) of the attenuated waveforms can be determined from

$$RL = L_p - \alpha r, \quad \alpha = \text{attenuation (dB}/\lambda), \quad r = \text{range (m)},$$

$$L_p = \text{sound-pressure level of the unattenuated waveform (dB)}.$$

Results:

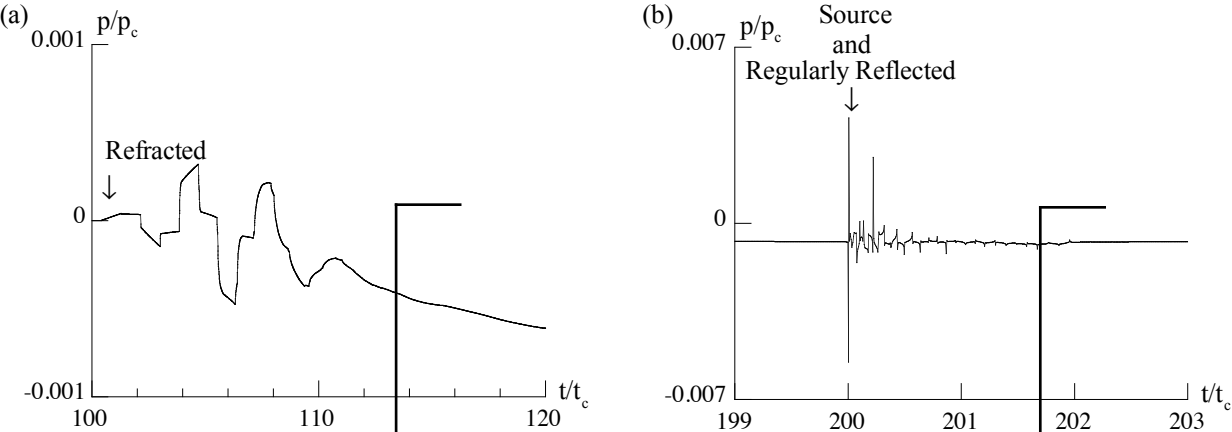


Fig. 2 Time records of the received unattenuated pressure due to a source signal of the form of a Heaviside unit function; (a) the critically refracted (lateral) waves; (b) the source signal and the regularly reflected waves; (c) the Scholte interface waves (t = time; p = pressure; t_c, p_c = normalizing constants).

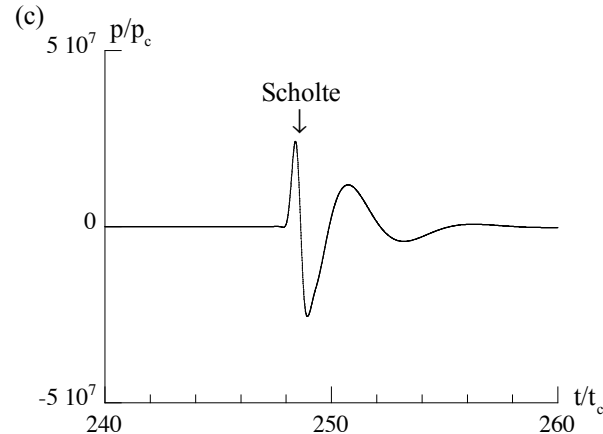


Fig. 2 – continued

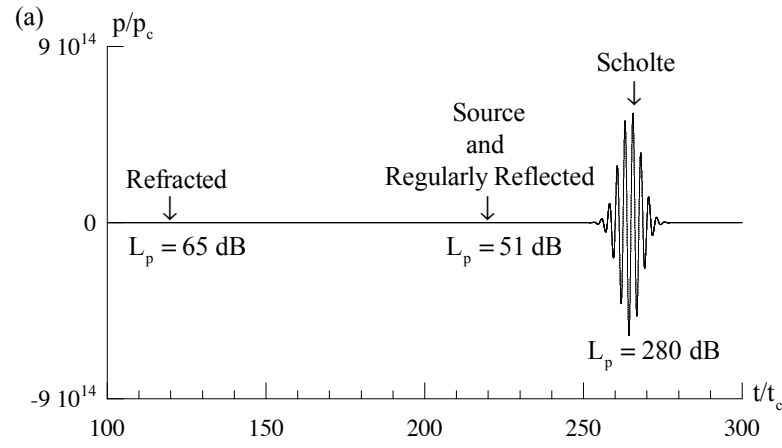


Fig. 3 Time record of the received unattenuated pressure due to a Gaussian-weighted source signal with a center frequency of $c_f = 3$ Hz, a bandwidth of $w = 0.5$ Hz, and a sound-pressure level of 171 dB re $1 \mu\text{Pa}$ at 1 m; (a) the entire record; (b) the early portion of the pressure curve shown in greater detail (t = time; p = pressure; t_c, p_c = normalizing constants, L_p = sound-pressure level). (b) on p. 4.

- INTRODUCTION
- OBJECTIVES
- METHODS/DATA
- RESULTS
- CONCLUSION



Please do not use this space, a QR code will be automatically overlaid

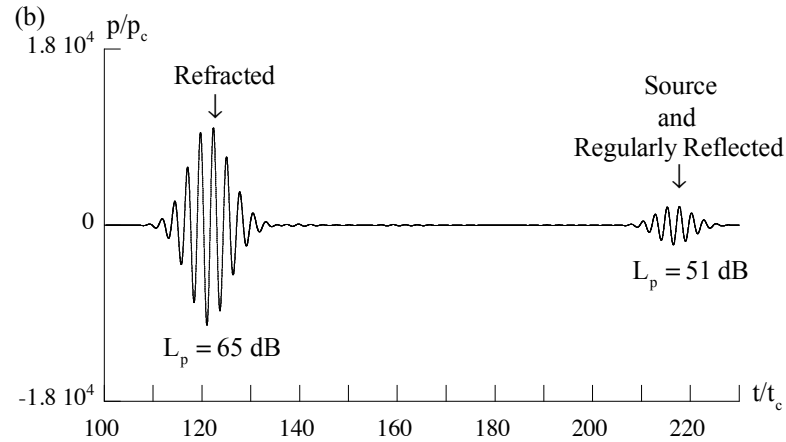


Fig. 3 – continued

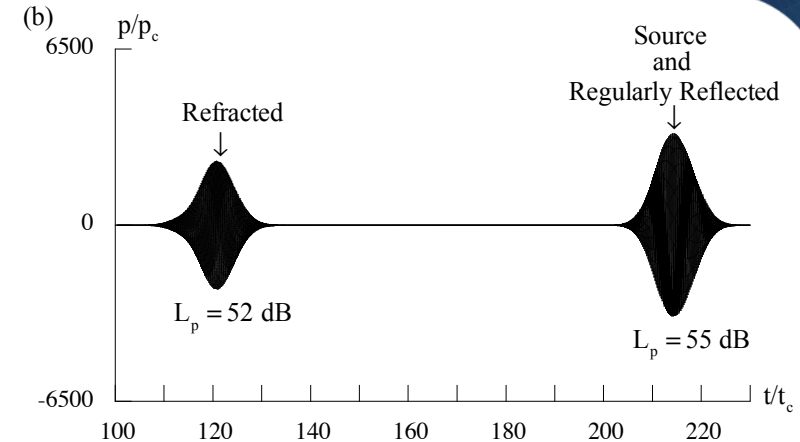
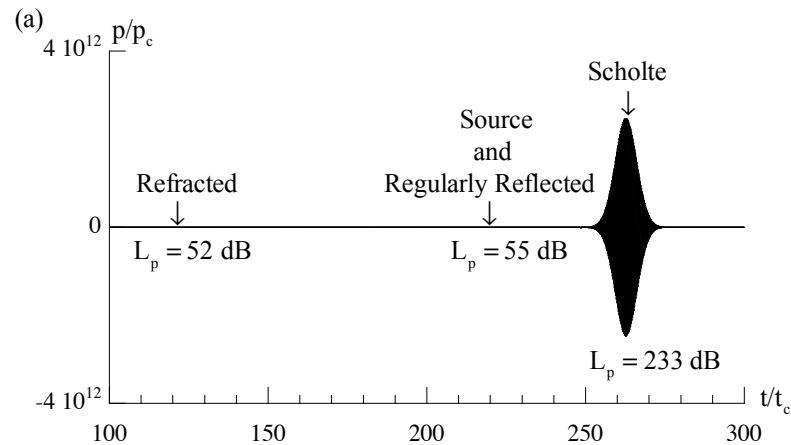


Fig. 4 – continued

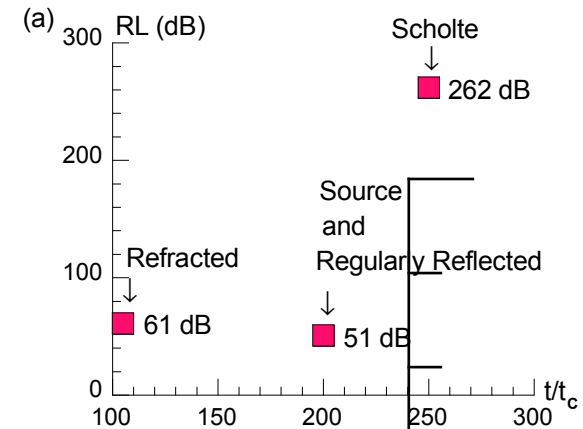


Fig. 5 Received levels (RLs) of the three (critically refracted, source signal and regularly reflected, and Scholte) attenuated waveforms, recorded in order of their arrivals at the receiver shown in Fig. 1; (a) due to a Gaussian-weighted source signal with a center frequency of $c_f = 3$ Hz, a bandwidth of $w = 0.5$ Hz, and a sound-pressure level of 171 dB re $1 \mu\text{Pa}$ at 1 m; continued on p.5.

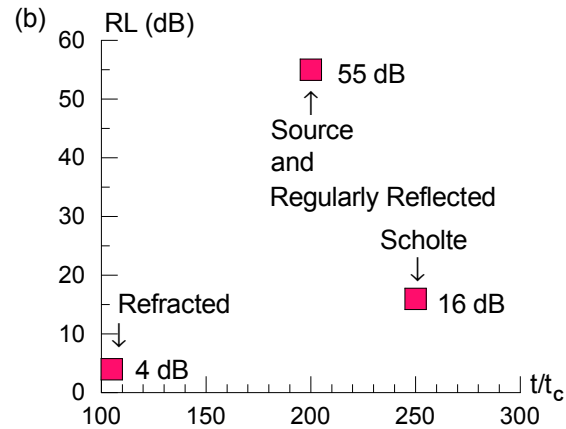


Fig. 5 – *continued* – (b) due to a Gaussian-weighted source signal with a center frequency of $c_f = 36$ Hz, a bandwidth of $w = 0.5$ Hz, and a sound-pressure level of 171 dB re 1 μ Pa at 1 m.

Conclusion:

1. When a source emits signals of a low-frequency content, like of 3 Hz [Fig. 5(a)], the contribution from the Scholte waves becomes dominant at large distances. Hence, low frequency long-range propagation in a shallow-water wedge (coastal wedge) over an elastic seabed may indeed be governed by the Scholte waves.
2. With the recent advent of a novel high order Gauss-Legendre quadrature [3] and benefits offered by High-Performance-Computing (HPC) environments, it can be possible in a reasonable time to achieve desired accuracy in the calculations, even at larger propagation ranges than those reported in the paper, by increasing the number of Gaussian points in numerical integration.

References:

[1] Hovem J.M. and Korakas A., *Marine Technology Society Journal*, Vol. **48**, pp. 72-80, 2014.
 [2] Borejko P., Chen C.F., and Pao Y.H., *J. Comput. Acoust.*, Vol. **9**, pp. 41-68, 2001.
 [3] Townsend A., *SIAM News*, Vol. **48**, pp. 1-3, 2015.



INTRODUCTION

OBJECTIVES

METHODS/DATA

RESULTS

CONCLUSION



Please do not use this space, a QR code will be automatically overlaid

P1.3-267